

Expression profile and histological distribution of IFITM1 and IFITM3 during H9N2 avian influenza virus infection in BALB/c mice

Meng Yu · Wenbao Qi · Zhiqiang Huang · Kaizhao Zhang · Jinhui Ye · Rongchang Liu · Heng Wang · Yongjiang Ma · Ming Liao · Zhangyong Ning

Received: 23 April 2014 / Accepted: 24 September 2014 / Published online: 30 September 2014
© Springer-Verlag Berlin Heidelberg 2014

Abstract The H9N2 avian influenza virus is a pandemic threat which has repeatedly caused infection in humans and shows enhanced replication and transmission in mice. Previous reports showed that host factors, the interferon-inducible transmembrane (IFITM) protein, can block the replication of pathogens and affect their pathogenesis. BALB/c mice are routine laboratory animals used in influenza virus research, but the effects of H9N2 influenza virus on tissue distribution and expression pattern of IFITM in these mice are unknown. Here, we investigated the expression patterns and tissue distribution of IFITM1 and IFITM3 in BALB/c mice by infection with H9N2 AIV strains with only a PB2 residue 627 difference. The results showed that the expression patterns of IFITM1 and IFITM3 differ in various tissues of BALB/c mice at different time points after infection. IFITM1 and IFITM3 showed cell- and tissue-specific distribution in the lung, heart, liver, spleen, kidney and brain. Notably, the epithelial and neuronal cells all expressed the proteins of IFITM1 and IFITM3. Our results provide the first look at differences in IFITM1 and IFITM3 expression patterns in BALB/c mice infected by H9N2 influenza viruses. This will enhance research on the

interaction between AIV and host and further will elucidate the pathogenesis of influenza virus infection based on the interferon-inducible transmembrane (IFITM) protein.

Keywords Avian influenza virus · H9N2 · IFITM1 · IFITM3 · BALB/c mice

Introduction

The H9N2 influenza virus is a pandemic threat according to the World Health Organization (WHO). Since the H9N2 subtype avian influenza virus (AIV) was first isolated and characterized in 1966 in turkeys [1], birds, including wild birds and domestic poultry populations, became the main victims of this virus [2–5]. This subtype AIV occurred mainly in Asia causing low mortality and immunosuppression in chickens and a decline in egg production [6, 7]. The Middle East, Africa and other non-Asian countries also reported outbreaks [5, 8, 9]. Recently, reports showed that this subtype of avian influenza virus has been transmitted from birds to dogs and cats, pigs and non-primate animals [10–13]. More importantly, the human cases of H9N2 influenza virus infection occurred with the clinical signs of mild respiratory tract inflammation in China [14]. The seroprevalence of avian influenza H9N2 in humans showed that it is trending toward a more prevalent pathogen in human populations [15]. The most important feature of this subtype AIV is that it provided the inner genes to other AIV types to form a new epidemic influenza virus. Reports showed that the avian influenza virus H9N2 provided its six inner genes to H7 subtype to form a new H7N9 virus which can infect and kill humans [16]. The latest H10N8 virus, which can be fatal to humans, also includes six inner genes of H9N2 [17]. There are evidences showed that the H9N2

Meng Yu, Wenbao Qi have contributed equally to this work.

Electronic supplementary material The online version of this article (doi:10.1007/s00430-014-0361-2) contains supplementary material, which is available to authorized users.

M. Yu · W. Qi · Z. Huang · K. Zhang · J. Ye · R. Liu · H. Wang · Y. Ma · M. Liao (✉) · Z. Ning (✉)
College of Veterinary Medicine, South China Agricultural University, Guangzhou 510642, People's Republic of China
e-mail: mliao@scau.edu.cn

Z. Ning
e-mail: ningzhyong@scau.edu.cn

avian influenza virus can, as reassortants, give its PB1 [18] or non-structure (NS) gene [19] to high pathogenic H5N1 AIV. H9N2 often co-exists and co-circulates with the other AIV types during their prevalence, such as its coexistence with the H7N9 [20] and H5N1 [4].

The mechanism regarding enhanced pathogenicity of the H9N2 virus in mice is still less known and remains to be determined [21]. Our previous reports showed that a single amino acid substitution in PB2 residue 627 changed the virulence of H9N2 avian influenza virus in mice [22, 23]. Similar to most pathogens, the clinical course induced by influenza virus was determined by the struggle between the virulence of the virus and the reaction of the host. To date, the host factors which play the role against the H9N2 subtype influenza virus is still obscure. The interferon-inducible transmembrane (IFITM) protein families are activated in response to viral infections and represent a new class of cellular restriction factors that block the replication of pathogens and its pathogenesis [24]. The average size of IFITM proteins including IFITM1–IFITM5 are 130 amino acids and share a topology defined by a conserved CD225 domain [24, 25], consisting of two intramembrane (IM) regions and a conserved intracellular loop (CIL). One or more IFITM proteins can be constitutively expressed in specific cells and tissues [25], such as a wide range of human tissues expressing IFITM1–IFITM3, while IFITM5 is expressed only in osteoblasts [26]. Potentially, this constitutive expression pattern of IFITM can provide the first line of defense against virus infection [26]. Increasingly, reports showed that IFITM offers protection against numerous viruses, including Influenza A, Rift Valley fever virus, SARS coronavirus, filoviruses, Dengue and HIV, through several routes, including inhibiting formation of a fusion pore between the virus and endosomal membranes [26–29]. In mouse models, IFITM3 has been shown to have the most antiviral activity of the IFITM class for the viruses investigated and restricted in influenza A virus infection [30]. IFITM1 also showed antiviral activity against Influenza A and hepatitis C virus [31, 32]. When the infection of influenza virus occurred, the expression profile of IFITM1 and IFITM3 and histological distribution are not clear.

In this research, we detected and examined the expression profile and histological distribution of IFITM1 and IFITM3 in tissues of the lung, heart, liver, spleen, kidney and brain during infection in BALB/c mice by H9N2 avian influenza virus strains only with difference at site 627 in PB2. This would allow us to generate basic data regarding IFITM1 and IFITM3 in H9N2 infection and further understand the role of PB2 residue 627 in the pathogenesis of H9N2 in mammalian hosts. To date, this is the first paper which shows the relationship between H9N2 avian influenza virus and the host factors, IFITM1 and IFITM3, in mice.

Materials and methods

Ethics statement

The animal experiments were approved by the Institutional Animal Care and Use Committee at the South China Agricultural University (Certification Number: CNAS BL0011) and performed in accordance with the “Guidelines for Experimental Animals” of the Ministry of Science and Technology (Beijing, China) and in association for Assessment and Accreditation of Laboratory Animal Care International-accredited facility.

Viruses and BALB/c mice infection by H9N2 influenza virus

The viruses used in this research were H9N2 AIVs, A/chicken/Guangdong/V/2008 (V_{K627}) and a site-mutation virus (rV_{K627E}), which were rescued by eight-plasmid reverse genetic system [22, 23]. When the mice were inoculated with 10^6 EID₅₀ V_{K627} , they will dead at 6 dpi [23], but mice only showed the greatest signs of illness, such as ruffled fur and severe morbidity (weight loss as a measure of morbidity) were inoculated with 10^4 PFU of V_{K627} [22]. Compared with V_{K627} , rV_{K627E} showed low pathogenicity and is non-lethal to mice [22, 23]. So, in this research, the mice were inoculated with 10^4 PFU of V_{K627} or rV_{K627E} . Thirty-six SPF female BALB/c mice (18.0–20.0 g, 6–8 weeks) from the Guangdong Experimental Animal Centre (Guangzhou, China) were randomly divided into three groups and set for sampling three every group every time point. After being anesthetized with CO₂, the mice were inoculated intranasally with 50 μ l of sterile, endotoxin-free PBS containing 10^4 PFU of V_{K627} or rV_{K627E} influenza virus; the mice in control were treated only by PBS. All mice were weighed before challenging and surveyed for daily weight loss as a measure of morbidity.

At 1, 3, 5 and 6 days post-inoculation (dpi), the lungs, hearts, livers, spleens, kidneys and brains of three euthanized mice in the infected and control groups, respectively, were collected promptly. Each tissue was divided into two parts. One part was frozen in liquid nitrogen for 2 h before storage at -86 °C for RNA extraction, and the other was fixed in 10 % neutralized buffered formalin for histopathological and immunohistochemical detection.

RNA extraction, cDNA preparation and real-time PCR

Total RNA of all samples was extracted, treated and quality determined as our previous report [33] and stored at -86 °C. Total RNA was reverse-transcribed to cDNA using PrimeScript RT reagent Kit (Takara Biotech, Dalian, China). Relative expression levels of IFITM1

and IFITM3 were determined by real-time PCR using DNA Engine 7500 Continuous Fluorescence Detection System (Applied Biosystems, CA, USA) and SYBR® Premix Ex Taq™ Kit (Takara Biotech, Dalian, China). Primers were designed for IFITM1, IFITM3 and β -actin based on the sequences from the database (accession no: NM_026820.3, NM_025378.2 and NM_007393.3). The primer sequences were synthesized as follows: 5'-GAA-GATGGTGGGTGATACGA-3' (IFITM1-Fw), 5'-G CAG CGATAGACAAGGAAAC-3' (IFITM1-Rv), 5'-GCC CCCAACTACGAAAGA-3' (IFITM3-Fw), 5'-ATTGAA CAGGGACCAGACCAC-3' (IFITM3-Rv), 5'-CATCCGTA AAGACCTCTATGCCA-3' (β -actin-Fw) and 5'-ATGGAGCC ACCGATCCACA-3' (β -actin-Rv). The melting curves for each PCR were carefully analyzed to avoid nonspecific amplifications in PCR products. The relative expression level of IFITM1 and IFITM3 was calculated by normalizing the levels of gene transcripts to that of β -actin transcripts using a relative standard curve method through $2^{-\Delta\Delta Ct}$ formula. Data were analyzed using GraphPad Prism 5 (GraphPad Software, La Jolla, CA). One-way ANOVA was used to determine statistical significance between samples in relative expression levels of IFITM1 and IFITM3. A $P < 0.05$ was considered to be statistically significant, while a $P < 0.01$ was considered to be highly significant.

Histopathological and immunohistochemical detection

Serial sections were taken from the same samples, one for histopathological observation using the routine HE staining and the other three for immunohistochemical detection. Immunohistochemical staining was performed as described in our previous publication [34]. Briefly, endogenous peroxidase activity was quenched using freshly prepared 3 % hydrogen peroxide for 15 min at ambient temperature and washing 3 times with 0.02 M PBS (pH = 7.2) at 5 min intervals. Antigen retrieval was performed using high-pressure method at 100 centigrade for 10 min before cooling naturally. After being washed 3 times by PBS at 5 min intervals, the samples were incubated with sheep serum for 10 min at ambient temperature. The slices then were incubated with the corresponding antibodies (IFITM1, ABBIO-TEC, USA, Cat.No., 251403 and IFITM3, PROTEINTECH GROUP INC, USA, Cat.No., 11714-1-AP) and their control for 1.5 h at 37 °C according with the manufactures' guidelines. After incubation with the secondary antibody for 1.5 h at 37 °C, the slices were washed with PBS at 5-min intervals a total of 3 times. DAB (3, 3'-diaminobenzidine tetrahydrochloride) Kit (ZSGQ-BIO, China) was used for coloration. Slices were re-dyed with hematoxylin for 1 min and washed with running water for 10 min. Finally, the slices were dehydrated using graded ethanol, vitrified by dimethylbenzene and deposited in neutral balsam.

Results

Virulence of avian influenza virus H9N2 in Mice

The weight loss, clinical signs, mortality and virus isolation from tissues after inoculation with V_{K627} and rV_{K627E} avian influenza virus H9N2 in mice are similar to our previous reports [22, 23]. The histopathological changes in lungs and brains of mice in different groups are different between the two infection groups. For the lungs, there were mild interstitial pneumonia with more infiltration of immunological cells and shedding of bronchial epithelial cells in the bronchiole of the V_{K627} group than in the rV_{K627E} group on 3 dpi (Fig. 1a–c). The V_{K627} virus induced significant viral encephalitis with infiltration of microglia cells and lymphocytes around the small blood vessels on 5 dpi, whereas the rV_{K627E} virus showed results similar to the control (Fig. 1d–f).

Statistic analysis of relative expression level of IFITM1 and IFITM3 during infection

IFITM1 and IFITM3 were ubiquitously expressed in all the tissues examined in BALB/c mice, but the expression levels of them were differed in different tissues between the control and H9N2 AIV infection groups.

In the lung, the expression level of IFITM1 reached the highest point at 6 dpi for V_{K627} infection, while at 1 dpi for rV_{K627E} infection. The statistical analysis showed that the expression level of IFITM1 for rV_{K627E} infection was very significantly higher than in the control ($P < 0.01$) and rV_{K627E} infection at 1 dpi and rV_{K627E} infection was significantly higher than in the control ($P < 0.05$) at this time point. However, at 3, 5 and 6 dpi, the expression level of IFITM1 was very significant higher in V_{K627} infection than in the rV_{K627E} infection and control ($P < 0.01$). At 6 dpi, the expression level of IFITM1 in the rV_{K627E} infection was very significantly higher than in the control ($P < 0.01$) (Fig. 2a). In the heart, the statistical analysis showed that the expression level of IFITM1 of the V_{K627} infection was very significantly higher than in the control and the rV_{K627E} infection at 3 and 6 dpi ($P < 0.01$) and significantly higher than in the other two groups at 5 dpi ($P < 0.05$). At 3 dpi, the expression level of IFITM1 in the rV_{K627E} infection was very significantly higher than in the control ($P < 0.01$) (Fig. 2b). In the liver, the statistical analysis showed that the expression level of IFITM1 in the V_{K627} infection was very significantly higher than in the rV_{K627E} infection at 5 dpi ($P < 0.01$). Conversely, at 6 dpi, it was significantly higher in the rV_{K627E} infection than in V_{K627} infection ($P < 0.05$) (Fig. 2c). Expression levels in spleen showed a rising trend and reach

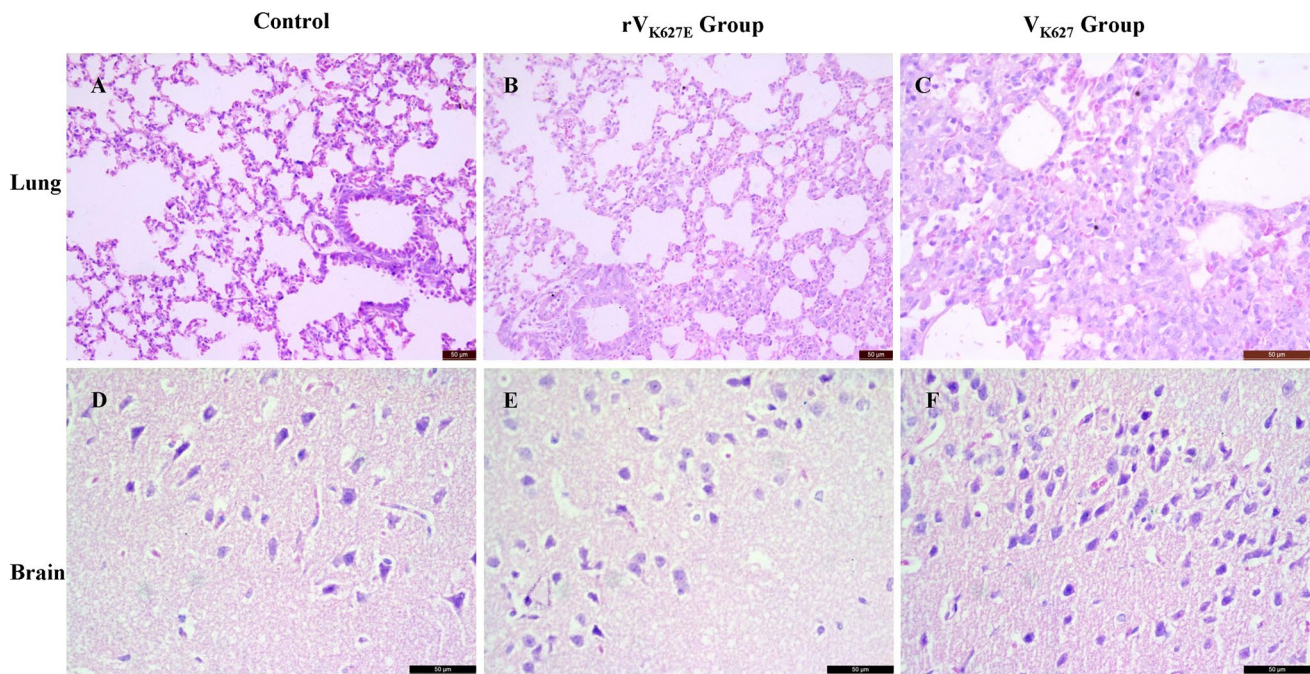


Fig. 1 Histopathological changes in lung (a, b and c) and brains (d, e and f) of mice in rV_{K627E} group, V_{K627} group and control

the highest point at 3 dpi for the V_{K627} infection, while it showed almost no significant change in the rV_{K627E} infection. The statistical analysis showed that, in spleen, the expression level of IFITM1 was very significant higher for the V_{K627} infection than in the rV_{K627E} infection and control at all detected time points ($P < 0.01$) (Fig. 2d). In the kidney, the statistical analysis showed that the expression levels of IFITM1 was very significant higher in the rV_{K627E} infection than in the V_{K627} infection and the control at 3 dpi ($P < 0.01$). At 5 dpi, it was significantly higher in the V_{K627} infection than in the rV_{K627E} infection ($P < 0.05$) and very significantly higher than in the control ($P < 0.01$). At 6 dpi, IFITM1 was very significantly higher in V_{K627} infection than in the other two groups ($P < 0.01$) (Fig. 2e). Finally, in the brain, the statistical analysis showed that the expression level of IFITM1 was very significantly higher in the rV_{K627E} infection than in the other two groups at 3, 5 and 6 dpi ($P < 0.01$). However, at 1 dpi, it was very significant higher than in the control ($P < 0.01$) but no difference with the V_{K627} infection (Fig. 2f).

In the lung for the V_{K627} infection, the expression levels of IFITM3 were similar to IFITM1 that was seen for the rV_{K627E} infection in lung. Meanwhile, for the rV_{K627E} infection, expression showed declining trend from 1 to 6 dpi. The statistical analysis showed that the expression level of IFITM3 in the rV_{K627E} infection was very significant higher than in the V_{K627} infection and the control ($P < 0.01$) and it was significantly higher in the V_{K627}

infection than in the control ($P < 0.05$) at 1dpi. It was significantly lower in the control than in the infected groups ($P < 0.01$) at 3 dpi. It was significantly higher for the rV_{K627E} infection than in the control at 5 dpi ($P < 0.05$). At 6 dpi, the expression levels of IFITM3 were very significantly higher in the V_{K627} infection than in the rV_{K627E} infection and the control ($P < 0.01$) (Fig. 2g). For the heart, the statistical analysis showed that the expression level of IFITM3 in the V_{K627} infection was significantly higher than in the control and the rV_{K627E} infection at 1 dpi ($P < 0.05$) and very significantly higher than in the other two groups at 5 and 6 dpi ($P < 0.01$). At 3 dpi, the expression level of IFITM3 in the control was very significantly lower than in the infection groups ($P < 0.01$). At 5 and 6 dpi, the expression level of IFITM3 in the rV_{K627E} infection was very significantly higher than in the control ($P < 0.01$) (Fig. 2h). In the liver, the statistical analysis showed that, at 1 dpi, the expression level of IFITM3 in V_{K627} infection was very significantly higher than in the control ($P < 0.01$) and rV_{K627E} infection was significantly higher than in the control ($P < 0.05$). At 3, 5 and 6 dpi, the expression level of IFITM3 in the control was very significantly lower than in the infected groups ($P < 0.01$) (Fig. 2i). In the spleen, the expression level of IFITM3 reached its highest point at 3 dpi for the V_{K627} and rV_{K627E} infection. The statistical analysis showed that the expression level of IFITM3 in the V_{K627} infection was significantly higher than in the control and rV_{K627} infection ($P < 0.05$) at 3, 5 and 6 dpi (Fig. 2j). In the kidney,

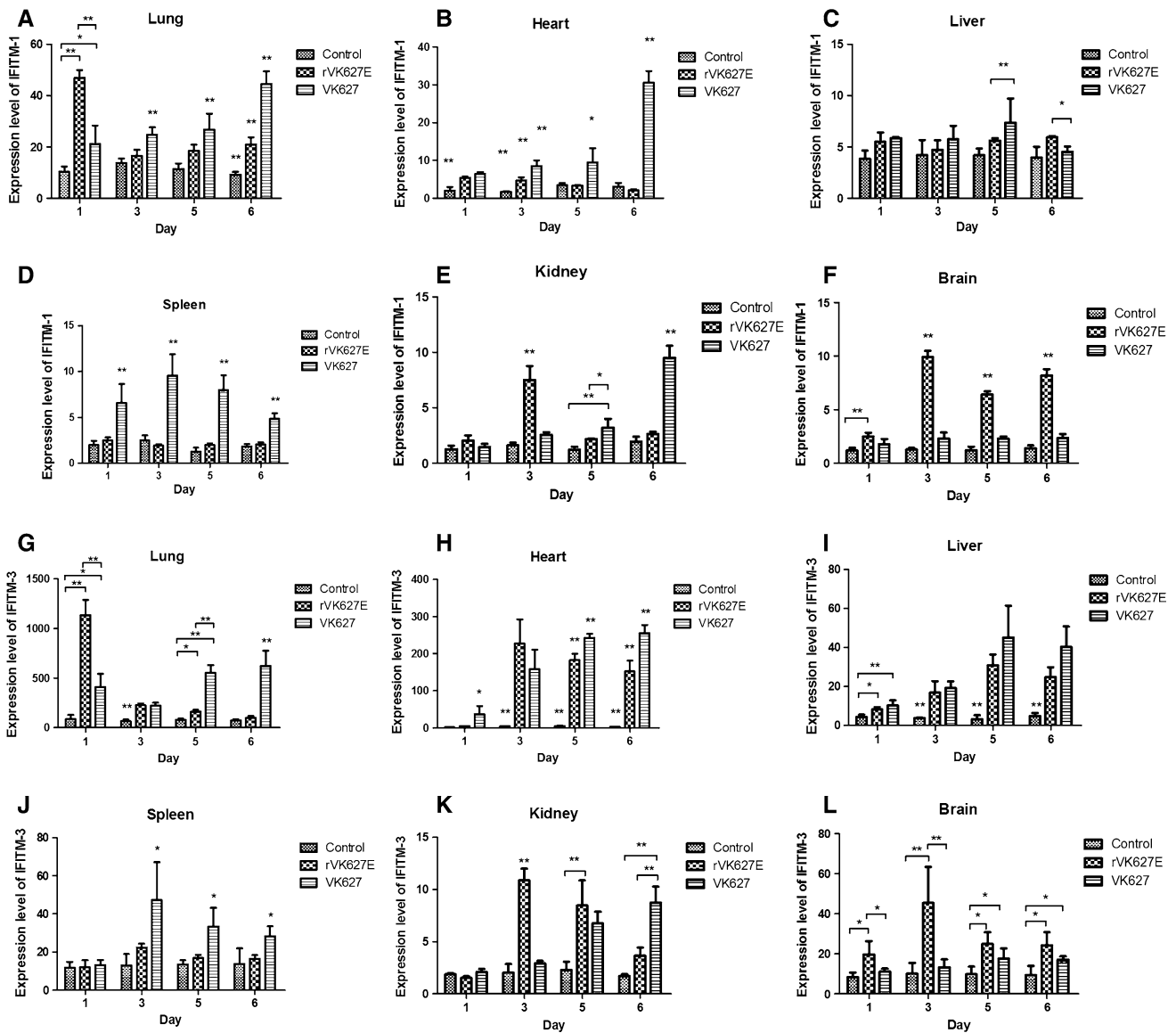


Fig. 2 Relative mRNA expression levels of IFITM1 and IFITM3 in the detected tissues of the control, rV_{K627E} and V_{K627} groups at different time points. * $P < 0.05$; ** $P < 0.01$. Data are represented as mean \pm standard deviation (SD). All samples were detected in triplicate

the statistical analysis showed that the expression level of IFITM3 in the rV_{K627} infection was very significantly higher than in rV_{K627E} infection and the control ($P < 0.05$) at 3 dpi, but at 5 dpi it is significantly higher in rV_{K627E} than in the control ($P < 0.01$). At 6 dpi, the expression level of IFITM3 in rV_{K627E} infection was very significantly higher than in rV_{K627} infection and the control ($P < 0.05$). (Fig. 2k). In brain, the statistical analysis showed that IFITM3 in the rV_{K627E} infection was significantly higher than in the other two groups ($P < 0.05$) at 1 dpi and was very significantly higher than in V_{K627} infection ($P < 0.01$) at 3 dpi. At 5 and 6 dpi, the expression level of IFITM3 of the infection group was significantly higher than in the control ($P < 0.05$) (Fig. 2l).

Tissue distribution of IFITM1 and IFITM3 detected by immunohistochemistry

Immunohistochemical detection was performed to show the distribution of the IFITM1 and IFITM3 proteins in the tissues of infected and control mice (Figs. 3, 4). In the lung, the IFITM1 positive cells are mainly the epithelial cells of the pulmonary alveoli in the control group mice, while both V_{K627}- and rV_{K627E}-infected mice all showed stronger positives in the epithelial cells of the pulmonary alveoli as well as the epithelial cells and the submucosa of bronchi and bronchioles. Notably, the shed bronchial epithelial cells, intraluminal secretions and infiltration cells in the alveolar wall and around the bronchi and bronchioles are strong

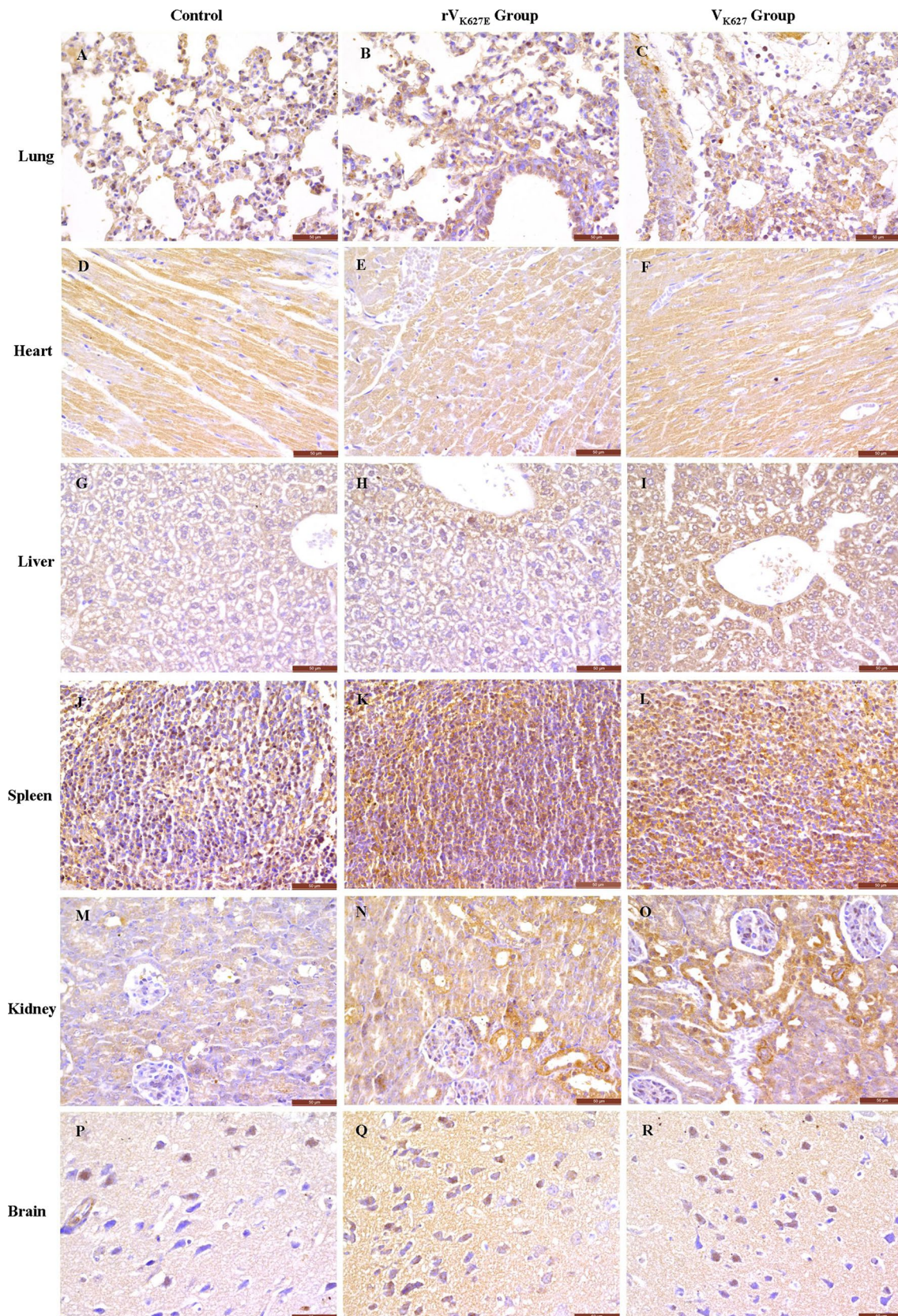


Fig. 3 Distribution of IFITM1 in the tissues of infected and control BALB/c mice at 5 dpi. Scale bar 50 μ m

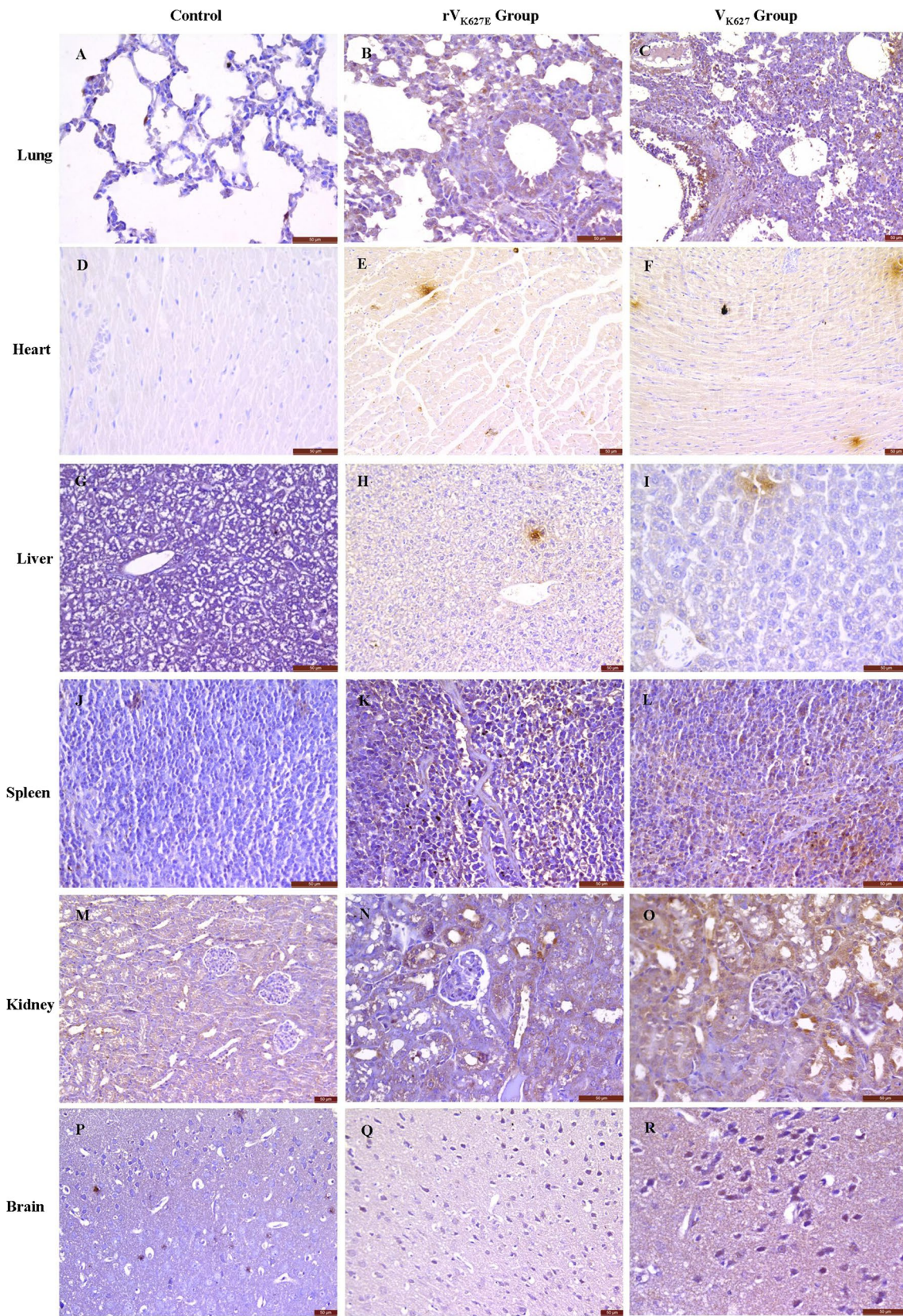


Fig. 4 Distribution of IFITM3 in the tissues of infected and control BALB/c mice at 5 dpi. Scale bar 50 μ m

positives (Fig. 3a–c). The distribution, in the lungs, of IFITM3 positive cells is similar to that of IFITM1 (Fig. 4a–c). For the heart, whether the myocardial cells were in the control, V_{K627} or rV_{K627E} group, all showed positive for IFITM1 (Fig. 3d–f). The IFITM3 in the muscle cells of the heart was negative in the control group, but positive cells are distributed in the infected groups, with the V_{K627} infection group having more positive focal distribution than the rV_{K627E} infection group (Fig. 4d–f). A similar situation occurred in the liver, but no difference between V_{K627} and rV_{K627E} infection groups was seen for IFITM3 (Fig. 4g–i). Meanwhile the liver cells of the control group were positive for IFITM1 in the cell membrane. The control and the rV_{K627E} groups are similar except that the strong positive cells are concentrated around the central vein in the rV_{K627E} group. All liver cells showed strong positive for IFITM1 in the V_{K627} group (Fig. 3g–i). In the spleen, the IFITM1 positive cells are diffusely distributed in the whole splenic corpuscle for the control group, but the V_{K627} and rV_{K627E} groups have more positive cells (Fig. 3j–l). For IFITM3 expression, the focal lymphocytes in the splenic corpuscle are positive and there are more lymphocytes which showed as stronger positives in the infected groups. Reticuloendothelial cells also showed strong positives in the infected groups but are negative in mice of the control group (Fig. 4j–l). In the kidney, the endothelial cells of some renal tubules were moderately positive for IFITM1 and IFITM3 and some cells in the glomerulus were positive for IFITM1. There were more strongly positive endothelial cells of the renal tubules in the V_{K627} group than in the rV_{K627E} group for both IFITM1 and IFITM3 (Figs. 3, 4m–o). Notably, some cells in the glomerulus were more positive in the V_{K627} and rV_{K627E} groups than in the control group for IFITM1 (Fig. 3m–o). In the brain, some of the cortical neurons showed moderately positive for IFITM1 with the infected groups having more strongly positive neurons, especially strongly positive infiltrated glial cells (Fig. 3p–r). IFITM3 showed similar results as IFITM1 (Fig. 4p–r).

Discussion

Mice are the routine model animals for studying influenza virus, previous researches showed that H9N2 AIVs can cause severe respiratory disease in experimentally infected mice without prior adaptation is increasing [6, 22, 35]. However, the basic data about the expression profile and tissue-specific distribution about the host factors during H9N2 avian influenza virus infection still obscure. The PB2 residue 627 in H9N2 AIV, A/chicken/Guangdong/V/2008, is the factor to determine its virulence [22], its relationship with the host response also needs to be known. In

mouse models, both IFITM1 and IFITM3 show antiviral and restriction activity in IAV infection [30–32]. In this research, IFITM1 and IFITM3 showed different tissue-specific expression patterns during H9N2 influenza virus infection. The lung is the most important replication site of the avian influenza virus in mouse [30, 36, 37] and host IFITM restriction is the most critical antiviral factor. For 5 days after infection, which has been proved as an important replication stage for the H9N2 AIV viruses [22, 23], the expression of IFITM3 in V_{K627} infected samples is continuously increasing, while continuously decreasing in rV_{K627E} infected tissues, suggesting that the host antiviral response was consistent with the virus replication. The expression pattern of IFITM1 showed distinct differences compared with IFITM3 in the V_{K627} infection and showed a similar pattern in rV_{K627E} infection. The most obvious difference is that V_{K627} infection can induce non-suppurative encephalitis, while rV_{K627E} infection cannot [22, 23]. IFITM3 were at low expression levels in brain tissue infected with V_{K627} , but were significantly higher (3 dpi) when infected by rV_{K627E} . This may suggest that a glutamic acid residue (E) in position 627 stimulate a host antiviral response in the brain. In the other tissues, the expression patterns of IFITM1 and IFITM3 were different for the various tissues. In the clinical course, some of them showed pathological changes, such as very slight lymphocytic myocarditis seen only in V_{K627} infection. The results of distinct expression patterns of IFITM1 and IFITM3 are consistent with previous research [28–31]. This may be correlated with the expression trends of the IFITM1 and IFITM3 in infected course. In our research, we also detected the relative expression levels of IFITM2, which are much lower than IFITM1 and IFITM3, except for brain, where the expression pattern roughly follows the expression of IFITM3 (Fig. S1). In order to elucidate the role of IFITM1, IFITM2 and IFITM3 in the different tissues, further research will be required.

Results of immunohistochemical detection showed that IFITM1 and IFITM3 are constitutively expressed in specific cells and tissues and have a wide range in BALB/c mice [24–26, 38]. To our knowledge, this is the first data which provide the tissue distribution of IFITM1 and IFITM3 for normal and influenza virus-infected BALB/c mice. Because the high degree of similarity of IFITM2 and IFITM3 [39], polyclonal antibody raised against IFITM3 will also be recognize IFITM2. For the most of the tissues analyzed with low expression levels, the antibody of IFITM3 detected protein is very likely IFITM3, but in brain, it maybe IFITM2/IFITM3. For the cell- and tissue-specific distribution of IFITM3 in lung and spleen, our results are consistent with respiratory syncytial virus (RSV)-infected mice [40]. The results of immunohistochemical detection of the lung are consistent with those of

the previous report on acute influenza virus-infected mice [28]. The cell- and tissue-specific distribution of IFITM1 and IFITM3 in the BALB/c mouse model of influenza virus will help to elucidate the role of tissues which participate in influenza virus infection and the innate immunity of animals to some viral diseases.

Our data showing the tissue distribution and expression patterns of IFITM1 and IFITM3 in AIV-infected mice further supports that these proteins may play a crucial role in the physiological and pathological processes of influenza infection. The tissue-specific alterations of IFITM1 and IFITM3 in mice infected with AIVs will further elucidate the role of these proteins on the pathogenesis of AIV. These basic data will enhance research on the interaction of AIV and the host and allow in-depth examinations into the pathogenesis of influenza virus infection based on the interferon-inducible transmembrane proteins.

Acknowledgments This work was partially supported by Science and technology nova Program of Pearl River of Guangzhou, Development Program for Excellent Young Teachers in Guangdong Province, Program for National Broiler Industry (nycytx-42-G3-03), Natural Science Foundation of Guangdong Province (S2013010013041).

References

1. Homme PJ, Easterday BC (1970) Avian influenza virus infections. I. Characteristics of influenza A-turkey-Wisconsin-1966 virus. *Avian Dis* 14:66–74
2. Kawaoka Y, Chambers TM, Sladen WL, Webster RG (1988) Is the gene pool of influenza viruses in shorebirds and gulls different from that in wild ducks? *Virology* 163:247–250
3. Alexander DJ (2000) A review of avian influenza in different bird species. *Vet Microbiol* 74:3–13
4. Arafa AS, Hagag NM, Yehia N, Zanaty AM, Naguib MM et al (2012) Effect of cocirculation of highly pathogenic avian influenza H5N1 subtype with low pathogenic H9N2 subtype on the spread of infections. *Avian Dis* 56:849–857
5. Davidson I, Shkoda I, Golender N, Perk S, Lapin K et al (2013) Genetic characterization of HA gene of low pathogenic H9N2 influenza viruses isolated in Israel during 2006–2012 periods. *Virus Genes* 46:255–263
6. Guo YJ, Krauss S, Senne DA, Mo IP, Lo KS et al (2000) Characterization of the pathogenicity of members of the newly established H9N2 influenza virus lineages in Asia. *Virology* 267:279–288
7. Kim JA, Cho SH, Kim HS, Seo SH (2006) H9N2 influenza viruses isolated from poultry in Korean live bird markets continuously evolve and cause the severe clinical signs in layers. *Vet Microbiol* 118:169–176
8. Tombari W, Paul M, Bettaieb J, Larbi I, Nsiri J et al (2013) Risk factors and characteristics of low pathogenic avian influenza virus isolated from commercial poultry in Tunisia. *PLoS ONE* 8:e53524
9. Parker CD, Reid SM, Ball A, Cox WJ, Essen SC et al (2012) First reported detection of a low pathogenicity avian influenza virus subtype H9 infection in domestic fowl in England. *Vet Rec* 171:372
10. Zhang K, Zhang Z, Yu Z, Li L, Cheng K et al (2013) Domestic cats and dogs are susceptible to H9N2 avian influenza virus. *Virus Res* 175:52–57
11. Yu H, Zhou YJ, Li GX, Ma JH, Yan LP et al (2011) Genetic diversity of H9N2 influenza viruses from pigs in China: a potential threat to human health? *Vet Microbiol* 149:254–261
12. Zhang K, Xu W, Zhang Z, Wang T, Sang X et al (2013) Experimental infection of non-human primates with avian influenza virus (H9N2). *Arch Virol* 158:2127–2134
13. Krumbholz A, Lange J, Dürrwald R, Walther M, Müller TH et al (2014) Prevalence of antibodies to European porcine influenza viruses in humans living in high pig density areas of Germany. *Med Microbiol Immunol* 203:13–24
14. Cheng VC, Chan JF, Wen X, Wu WL, Que TL et al (2011) Infection of immunocompromised patients by avian H9N2 influenza A virus. *J Infect* 62:394–399
15. Coman A, Maftei DN, Krueger WS, Heil GL, Friary JA et al (2013) Serological evidence for avian H9N2 influenza virus infections among Romanian agriculture workers. *J Infect Public Health* 6:438–447
16. Liu D, Shi W, Shi Y, Wang D, Xiao H et al (2013) Origin and diversity of novel avian influenza A H7N9 viruses causing human infection: phylogenetic, structural, and coalescent analyses. *Lancet* 381:1926–1932
17. Chen H, Yuan H, Gao R, Zhang J, Wang D et al (2014) Clinical and epidemiological characteristics of a fatal case of avian influenza A H10N8 virus infection: a descriptive study. *Lancet* 383:714–721
18. Monne I, Yamage M, Dauphin G, Claes F, Ahmed G et al (2013) Reassortant avian influenza A(H5N1) viruses with H9N2-PB1 gene in poultry, Bangladesh. *Emerg Infect Dis* 19:1630–1634
19. Munir M, Zohari S, Iqbal M, Abbas M, Perez DR et al (2013) The non-structural (NS) gene segment of H9N2 influenza virus isolated from backyard poultry in Pakistan reveals strong genetic and functional similarities to the NS gene of highly pathogenic H5N1. *Virulence* 4:612–623
20. Yu X, Jin T, Cui Y, Pu X, Li J et al (2014) Influenza H7N9 and H9N2 viruses: coexistence in Poultry Linked to Human H7N9 infection and genome characteristics. *J Virol* 88:3423–3431
21. Doerr HW, Cinatl J (2012) Recent publications in medical microbiology and immunology: a retrospective. *Med Microbiol Immunol* 201:1–5
22. Tian J, Qi W, Li X, He J, Jiao P et al (2012) A single E627 K mutation in the PB2 protein of H9N2 avian influenza virus increases virulence by inducing higher glucocorticoids (GCs) level. *PLoS ONE* 7:e38233
23. Li X, Qi W, He J, Ning Z, Hu Y et al (2012) Molecular basis of efficient replication and pathogenicity of H9N2 avian influenza viruses in mice. *PLoS ONE* 7:e40118
24. Siegrist F, Ebeling M, Certa U (2011) The small interferon-induced transmembrane genes and proteins. *J Interferon Cytokine Res* 31:183–197
25. Chan YK, Huang IC, Farzan M (2012) IFITM proteins restrict antibody-dependent enhancement of dengue virus infection. *PLoS ONE* 7:e34508
26. Smith SE, Gibson MS, Wash RS, Ferrara F, Wright E et al (2013) Chicken interferon-inducible transmembrane protein 3 restricts influenza viruses and lyssaviruses in vitro. *J Virol* 87:12957–12966
27. Perreira JM, Chin CR, Feeley EM, Brass AL (2013) IFITMs restrict the replication of multiple pathogenic viruses. *J Mol Biol* 425:4937–4955
28. Huang IC, Bailey CC, Weyer JL, Radoshitzky SR, Becker MM et al (2011) Distinct patterns of IFITM-mediated restriction of filoviruses, SARS coronavirus, and influenza A virus. *PLoS Pathog* 7:e1001258
29. Brass AL, Huang IC, Benita Y, John SP, Krishnan MN et al (2009) The IFITM proteins mediate cellular resistance to influenza A H1N1 virus, West Nile virus, and dengue virus. *Cell* 139:1243–1254

30. Everitt AR, Clare S, Pertel T, John SP, Wash RS et al (2012) IFITM3 restricts the morbidity and mortality associated with influenza. *Nature* 484:519–523
31. Hach JC, McMichael T, Chesarino NM, Yount JS (2013) Palmitoylation on conserved and nonconserved cysteines of murine IFITM1 regulates its stability and anti-influenza A virus activity. *J Virol* 87:9923–9927
32. Wilkins C, Woodward J, Lau DT, Barnes A, Joyce M et al (2013) IFITM1 is a tight junction protein that inhibits hepatitis C virus entry. *Hepatology* 57:461–469
33. Tong S, Tian J, Wang H, Huang Z, Yu M et al (2013) H9N2 avian influenza infection altered expression pattern of sphingosine-1-phosphate receptor 1 in BALB/c mice. *Virol J* 10:296
34. Li H, Ning Z, Hao W, Zhang S, Liao X et al (2012) Identification and characterization of monoclonal antibodies against the ORFV059 protein encoded by Orf virus. *Virus Genes* 44:429–440
35. Bi J, Deng G, Dong J, Kong F, Li X et al (2010) Phylogenetic and molecular characterization of H9N2 influenza isolates from chickens in Northern China from 2007–2009. *PLoS ONE* 5:e13063
36. Reading PC, Pickett DL, Tate MD, Whitney PG, Job ER et al (2009) Loss of a single N-linked glycan from the hemagglutinin of influenza virus is associated with resistance to collectins and increased virulence in mice. *Respir Res* 10:117
37. Gao P, Watanabe S, Ito T, Goto H, Wells K et al (1999) Biological heterogeneity, including systemic replication in mice, of H5N1 influenza A virus isolates from humans in Hong Kong. *J Virol* 73:3184–3189
38. Mikedis MM, Downs KM (2013) Widespread but tissue-specific patterns of interferon-induced transmembrane protein 3 (IFITM3, FRAGILIS, MIL-1) in the mouse gastrula. *Gene Expr Patterns* 13:225–239
39. Zhao X, Guo F, Liu F, Cuconati A, Chang J et al (2014) Interferon induction of IFITM proteins promotes infection by human coronavirus OC43. *Proc Natl Acad Sci USA* 111:6756–6761
40. Everitt AR, Clare S, McDonald JU, Kane L, Harcourt K et al (2013) Defining the range of pathogens susceptible to Ifitm3 restriction using a knockout mouse model. *PLoS ONE* 8:e80723